Heliyon 7 (2021) e07147

Contents lists available at ScienceDirect

Heliyon

journal homepage: www.cell.com/heliyon

Research article

SARS-CoV-2 infection paralyzes cytotoxic and metabolic functions of the immune cells

Yogesh Singh [a,b,f,*,1], Christoph Trautwein [c,1], Rolf Fendel [d,1], Naomi Krickeberg [d], Georgy Berezhnoy [c], Rosi Bissinger [e], Stephan Ossowski [a,b], Madhuri S. Salker [f], Nicolas Casadei [a,b], Olaf Riess [a,b,**], and the Deutsche COVID-19 OMICS Initiate (DeCOI)[2]

[a] Institute of Medical Genetics and Applied Genomics, University of Tübingen, Calwerstrasse 7, 72076, Tübingen, Germany
[b] NGS Competence Center Tübingen (NCCT), University of Tübingen, Calwerstrasse 7, 72076 Tübingen, Germany
[c] Werner Siemens Imaging Center, University of Tübingen, Röntgenweg 13, 72076, Tübingen, Germany
[d] Institute of Tropical Medicine, University Hospital of Tübingen, Wilhelmstrasse 27, 72076, Tübingen, Germany
[e] Department of Internal Medicine, Division of Endocrinology, Diabetology and Nephrology, University Hospital of Tübingen, Germany
[f] Research Institute of Women's Health, University of Tübingen, Calwerstrasse 7/6, 72076, Tübingen, Germany

ARTICLE INFO

Keywords:
COVID-19
$CD8^+$ T cells
Granzyme A
Perforin
Metabolites
^{1}H-NMR
Flow cytometry

ABSTRACT

The SARS-CoV-2 virus is the causative agent of the global COVID-19 infectious disease outbreak, which can lead to acute respiratory distress syndrome (ARDS). However, it is still unclear how the virus interferes with immune cell and metabolic functions in the human body. In this study, we investigated the immune response in acute or convalescent COVID-19 patients. We characterized the peripheral blood mononuclear cells (PBMCs) using flow cytometry and found that $CD8^+$ T cells were significantly subsided in moderate COVID-19 and convalescent patients. Furthermore, characterization of $CD8^+$ T cells suggested that convalescent patients have significantly diminished expression of both perforin and granzyme A. Using ^{1}H-NMR spectroscopy, we characterized the metabolic status of their autologous PBMCs. We found that fructose, lactate and taurine levels were elevated in infected (mild and moderate) patients compared with control and convalescent patients. Glucose, glutamate, formate and acetate levels were attenuated in COVID-19 (mild and moderate) patients. In summary, our report suggests that SARS-CoV-2 infection leads to disrupted $CD8^+$ T cytotoxic functions and changes the overall metabolic functions of immune cells.

1. Introduction

The first cases of severe acute respiratory coronavirus-2 (SARS-CoV-2) infection appeared in December 2019, in Wuhan, China [1]. This zoonotic virus has infected by now more than 127.8 million people (30.03.2021) and has resulted in more than 2.78 million death worldwide [2, 3]. The containment of the pandemic is challenging and is still growing with roughly 200,000 or more new infections being reported daily since July 2020 [2,3]. There is an urgent need for a better understanding of the immunopathology, as SARS-CoV-2 has become the leading cause of morbidity (long COVID syndrome) and mortality in many countries.

Coronaviruses (CoV) are a large family of viruses that can cause illnesses such as the common cold and seasonal influenza [4]. Pathologically, SARS-CoV-2 typically infects *via* angiotensin-converting enzyme 2 (ACE2)-expressing nasal epithelial cells in the upper respiratory tract and type II alveolar epithelial cells in patients exhibiting pneumonitis [1, 5]. The most severe disease courses led frequently to death but, not exclusively in older patients with and without risk conditions. The primary symptoms of SARS-CoV-2 infections are fatigue, fever, sore throat, dry cough, loss of smell and taste within 5–21 days of incubation of the virus [6, 7, 8, 9]. COVID-19 symptoms are heterogeneous and range from asymptomatic to mild, moderate, and severe pathological symptoms, presenting with or without pneumonia [10, 11]. However, most infected

* Corresponding author.
** Corresponding author.
E-mail addresses: yogesh.singh@med.uni-tuebingen.de (Y. Singh), olaf.riess@med.uni-tuebingen.de (O. Riess).
[1] Equal contributions.
[2] The members of the the Deutsche COVID-19 OMICS Initiative (DeCOI) collaborators are listed at the Declaration of interests statement section.

https://doi.org/10.1016/j.heliyon.2021.e07147
Received 29 September 2020; Received in revised form 10 March 2021; Accepted 24 May 2021

people develop mild to moderate illness and recover without hospitalization [12, 13]. High serum levels of IL-6, IL-8, IL-10, TNF-α cytokines and an immune hyper-responsiveness referred to as a 'cytokine storm' is connected with poor clinical outcome [14, 15]. Predominantly, older COVID-19 patients can develop acute severe respiratory distress syndrome (ARDS) due to a cytokine storm which is a life-threatening situation, requiring ventilation and intensive care support [16, 17, 18, 19, 20].

Several breakthrough discoveries have extended our understanding as to how the virus takes advantage of the host and modulates immunity [12, 19, 21, 22, 23, 24, 25]. Recovered COVID-19 patients have an increased number of antibody-secreting cells and activated $CD4^+$ and $CD8^+$ T cells. Further, Immunoglobulin M (IgM) and SARS-CoV-2 reactive IgG antibodies were also detected in blood before full symptomatic recovery [26, 27, 28]. Most severely affected COVID-19 patients had a lower T cell but elevated B cell counts when compared with healthy controls [13, 14, 29, 30]. Interestingly, patients with mild symptoms were also shown to have increased T and B cells compared with severely affected patients [26, 29, 30, 31]. There could be several reasons for different disease outcomes including an over-activated innate or hyper-activated adaptive immune response leading to cytokine storms and resulting in severe injury to the lungs [10, 13, 25, 32]. Despite several ongoing efforts, the immunological mechanisms of the host-pathogen interaction are not well understood [33].

There is an intricate balance between the metabolic state of immune cells and the generation of a robust immune response [19, 34, 35, 36, 37]. $CD8^+$ T cells require energy to proliferate and accomplish their effective functions [38]. Most propagating cells such as lymphocytes utilize the most abundant energy substrates including, glucose, lipids and amino acids [39]. In response to SARS-CoV-2 and other virus infections, $CD8^+$ T cells play a pivotal role. They undergo profound growth and proliferation to generate their effective functional cells which can produce copious amounts of effector molecules such as cytokines and cytotoxic granules [30, 38, 39, 40]. An activated immune system is coupled with a change in metabolic reprogramming to produce enough energy needed during (viral) infection [38, 39]. Proliferating T cells ferment glucose to lactate even in the presence of oxygen to meet high energy demands [34, 37, 38, 39]. Furthermore, glucose and glutamine are involved in the hexosamine biosynthetic pathway, which regulates the production of uridine diphosphate N-acetyl glucosamine necessary for T cell clonal expansion and function [41]. The synthesis of lactate intracellularly is crucial for T cells to have an increased glycolytic flux [38].

Peripheral blood mononuclear cells (PBMCs) can be analyzed to measure the physiological dysfunctionality of an individual and can serve as a biomarker [42]. Consequently, the metabolic status of lymphocytes could help to predict disease severity or to select the optimal therapeutic intervention to boost the immune function during infection. Generally, most of the metabolism-related functions in PBMCs during SARS-CoV-2 infections were inferred based on transcriptomics analysis [34, 43] and no functional data (biochemical level) have been presented. Therefore, understanding the kinetics of the adaptive immune response as well as the metabolic functions during SARS-CoV-2 infection will help to elucidate the host immune response to SARS-CoV-2 infection. In this study, using flow cytometry and proton nuclear magnetic resonance (^{1}H-NMR) spectroscopy, we characterized the PBMCs from SARS-CoV-2 infected and convalescent patients for their immunophenotypic and metabolic functions.

2. Results

2.1. Characteristics of study participants

PBMCs were isolated and cryopreserved from blood samples obtained from COVID-19 patients suffering from mild ('Mild (outpatient)') or moderate/severe ('Moderate (inpatient)') disease or were already recovered ('Convalescent') and from healthy controls ('HC'). Classification of disease severity for this analysis was based on the requirement of hospitalization. Patients with mild COVID-19 were recruited within three days after confirmation of infection by RT-qPCR. From moderate to severe COVID-19 patient blood samples were collected one week after their hospital admittance. The moderate patients were admitted to the hospital requiring medical care; however, they did not need ventilation or O_2 supply. Recovered patients were included based on a positive SARS-CoV-2 antibody testing. Study participant characteristics are described in Table 1.

2.2. Immunophenotyping of COVID-19 mild, moderate and convalescent COVID-19 patients

To compare the number of lymphocytes and monocytes amongst the four study groups, PBMCs were stained and analysed by flow cytometry. Based on live-cell percentage count (gating strategy; Figure 1a), both, lymphocytes and monocytes were not significantly different among mild, moderate and convalescent COVID-19 patients compared with HC (Figure 1b-d).

2.3. Increased inflammatory monocytes and reduced NK cells in moderate COVID-19 patients

Monocytes were further classified into classical, non-classical and intermediate based on the expression of CD16 and/or CD14 and were gated as described earlier [44] (Figure 1a). We found that $CD16^+CD14^-$

Table 1. Patient demographics.

No	COVID-19 status	Blood sampling	COVID-19 severity	Sex	Age
1	Outpatient (mild)	Day 1	mild	F	21
2	Outpatient (mild)	Day 1	mild	M	59
3	Outpatient (mild)	Day 1	mild	F	40
4	Inpatient (moderate)	Day 7	Moderate	M	57
5	Inpatient (moderate)	Day 7	Moderate	M	47
6	Inpatient (moderate)	Day 7	Moderate	F	78
7	Convalescent (Sero +ve)	Convalescent	Recovered, healthy	F	50
8	Convalescent (Sero +ve)	Convalescent	Recovered, healthy	F	24
9	Convalescent (Sero +ve)	Convalescent	Recovered, healthy	M	50
10	Convalescent (Sero +ve)	Convalescent	Recovered, healthy	F	51
11	HC1	-	None	F	36
12	HC2	-	None	M	60
13	HC3	-	None	M	40
14	HC4	-	None	M	37
15	HC5	-	None	M	47

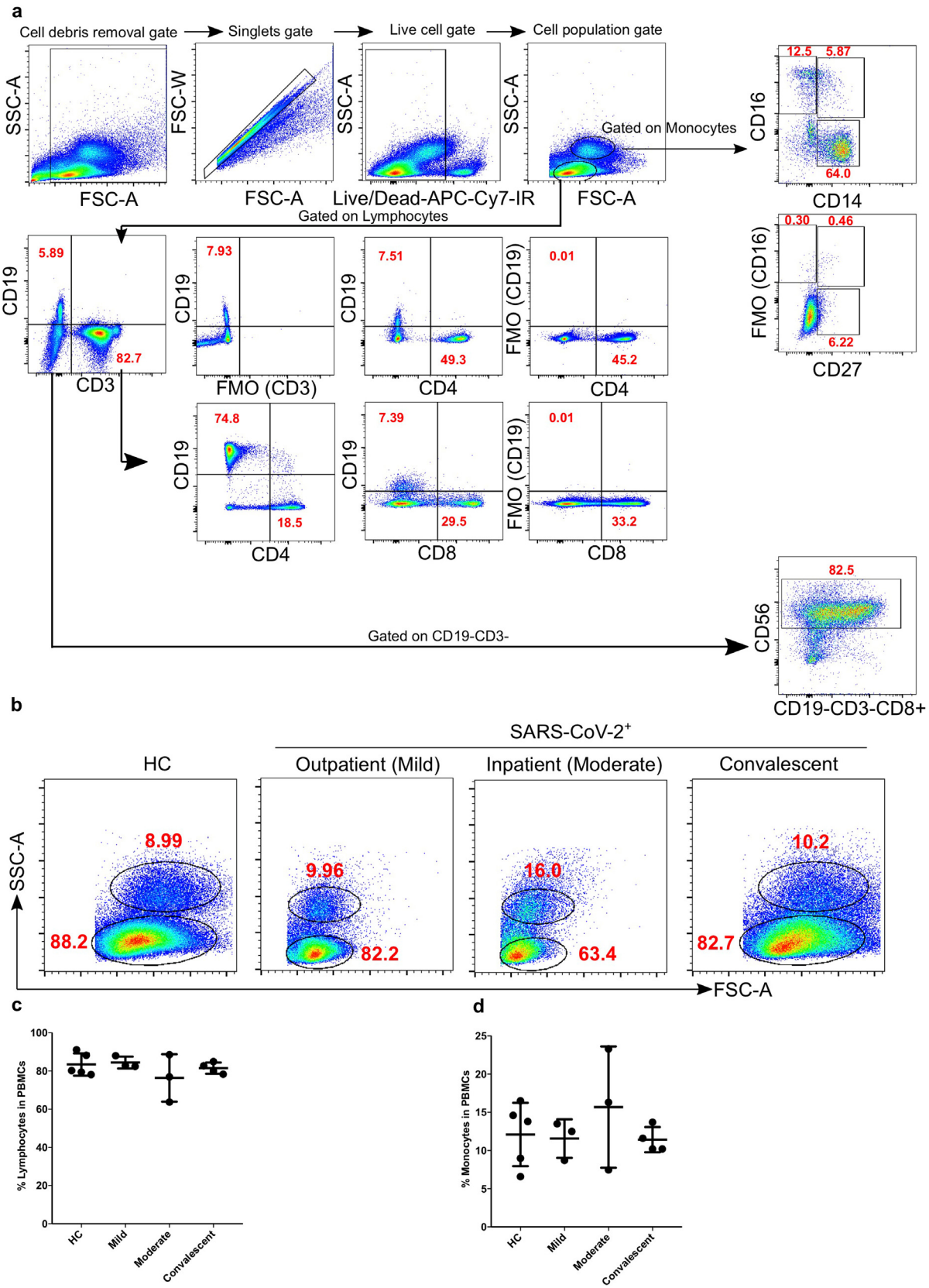

Figure 1. Total % counts of monocytes and lymphocytes from PBMCs of COVID-19 patients. a. Fixed PBMCs samples (1×10^6 cells) were collected and subsequently acquired on flow cytometry. A total of 200,000 cells were acquired by flow cytometry and gating was performed based on FSC and SSC parameters for lymphocytes, monocytes and dead cells as described earlier [76, 77, 78]. Gating strategy for T lymphocytes (CD3, CD4 and CD8) monocytes (CD14 and CD16) [44], NK cells (CD56) using FMO controls. b. The bar graphs represent the % of lymphocytes and monocytes. c–d. The representative gated lymphocytes and monocytes FACS plots. The bar graphs represent the % of lymphocytes and monocytes.

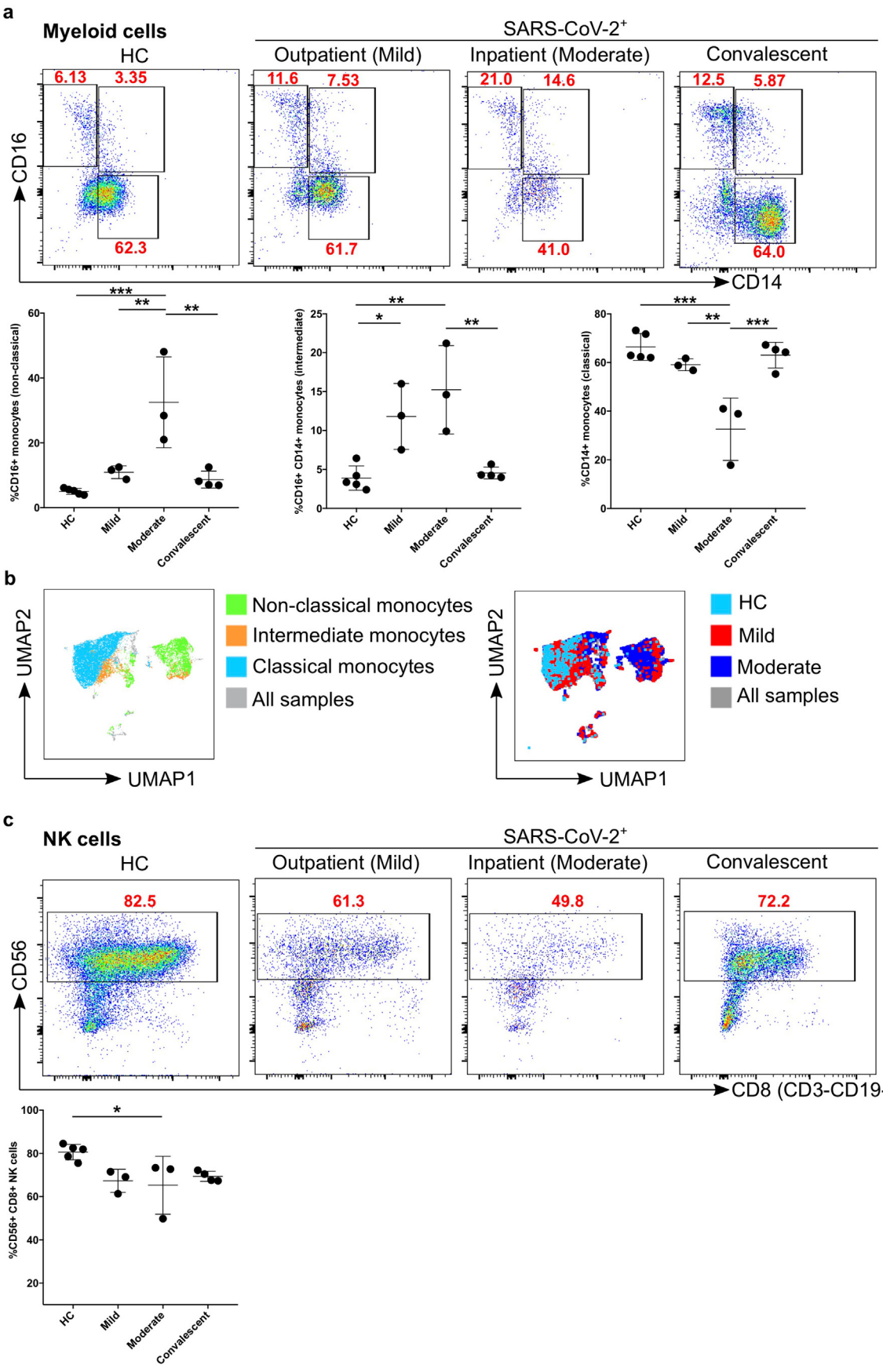

(caption on next page)

Figure 2. Comparison of monocytes and NK cell percentage amongst study groups. a. The stained PBMCs were gated on the monocyte population and $CD3^{+}CD19^{+}$ cells were excluded. Cell populations are displayed for CD16 and CD14 expression (upper FACS panel). One exemplary dot plot is shown per study group. The bar diagrams (lower panel) show the non-classical ($CD16^{+}CD14^{-}$), intermediate ($CD16^{+}CD14^{+}$) and classical ($CD16^{-}CD14^{+}$) monocytes. *P-value ≤0.05, **P-value ≤0.01 and ***P-value ≤0.001. b. UMAP plot for different subsets of monocytes (non-classical, intermediate and classical monocytes; left UMAP plot) from all the samples. Group comparisons among HC, mild and moderate (right UMAP plot). Colour-coded information is provided for either different subsets of monocyte populations or patient groups. c. The stained PBMCs were gated on lymphocyte population and further excluded the $CD3^{+}CD19^{+}$ cells and examined for the CD56 and CD8 expression in HC, mild, moderate and convalescent (upper FACS panel). One exemplary dot plot is shown per study group. The bar diagram shows the $CD56^{+}CD8^{+}CD3^{-}CD19^{-}$ NK cells. *P-value ≤0.05.

patrolling (non-classical) monocytes were significantly increased (p = 0.0004) in percentage in moderate patients compared to HC, whereas this number is decreased again significantly compared with convalescent patients (p = 0.001) (Figure 2a). The percentage of $CD16^{+}CD14^{-}$ (non-classical) monocytes was also significantly increased (p = 0.006) in moderate patients compared with mild patients (Figure 2a Panel I; left). Interestingly, $CD16^{+}CD14^{+}$ pro-inflammatory monocytes (intermediate) were again significantly increased in mild (p = 0.03) and moderate (p = 0.002) compared with HC as well as between moderate and convalescent (p = 0.005) (Figure 2a panel II; middle). Furthermore, we observed a significantly reduced percentage of $CD14^{+}CD16^{-}$ phagocytic monocytes (classical) in moderate compared with mild (p = 0.004), HC (p < 0.0002) and convalescent (p = 0.0007) patients (Figure 2a Panel III; right). Based on the results above using classical 2D flow cytometry analysis, we observed a major difference between HC *vs* mild or with moderate COVID-19 patient samples, therefore, we concatenated three groups together (equal number of cells from each sample; HC, mild and moderate) to identify the visual clustering of monocytes using Uniform Manifold Approximation and Projection (UMAP) for dimension reduction algorithm [45] (Figure 3). Based on UMAP dimension reduction analysis (data-driven and gated cells), we observed a clear difference in the different subsets of monocytes between all three groups (Figures 3c, d and 2b). We observed that moderate COVID-19 patients mostly cluster in non-classical and partially in intermediate monocyte regions compared to HC, whilst mild COVID-19 patients cluster in all non-classical, intermediate and classical monocytes regions (Figure 2b; right). We then explored the lymphoid cells compartment for NK cells ($CD56^{+}CD8^{+}CD3^{-}CD19^{-}$). We found that moderate patients were significantly different from HC (p = 0.04). There was also a tendency of a decrease in NK cells in mild patients compared with HC (p = 0.07), although, not reaching statistical significance (Figure 2c).

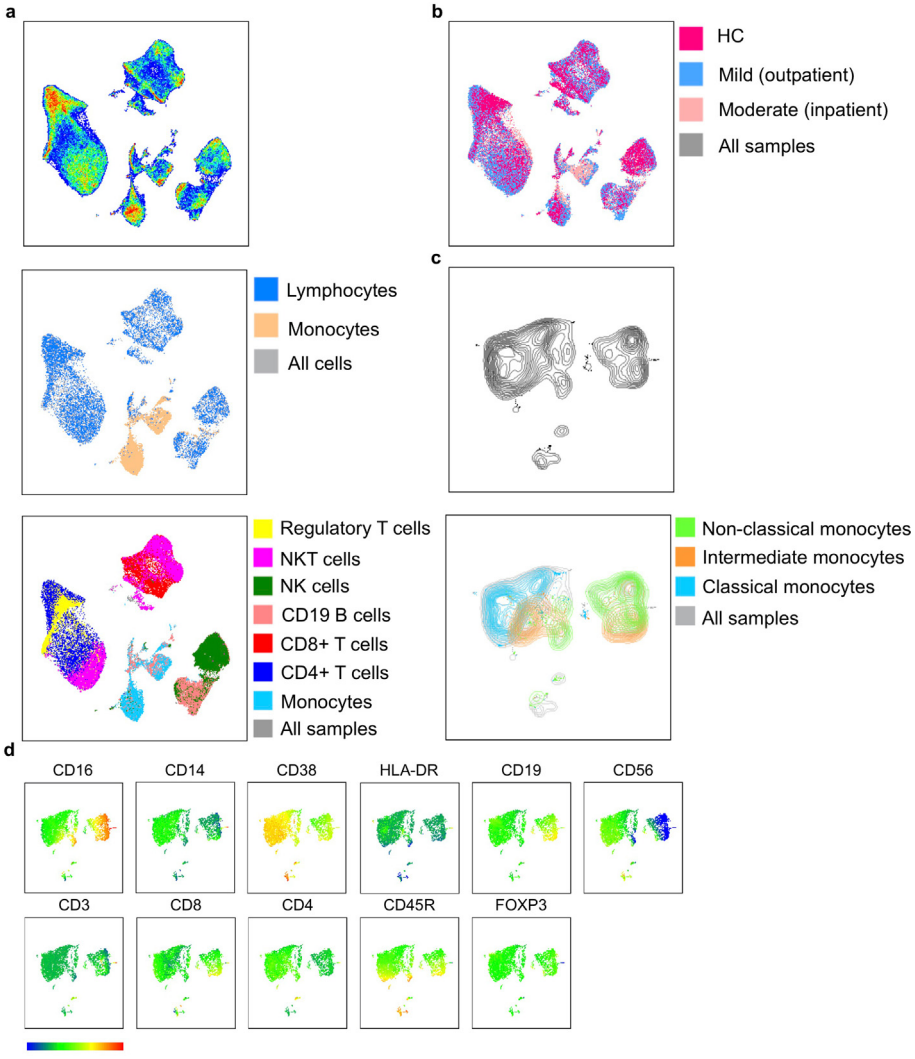

Figure 3. UMAP analysis of lymphocytes and monocytes cell populations. a. UMAP pseudo-colour plot was derived from all the samples. All the FCS files (used only live cell gated population; minimum cells per samples were 25,000) were concatenated from HC, mild and moderate patients (upper panel). Representation of lymphocytes and monocytes populations in UMAP plot (middle panel). Presentation of different lymphocytes subpopulations like $CD4^{+}$ T cells, $CD8^{+}$ T cells, B cells, NK cells, NKT cells and regulatory T cells (lower panel). b. UMAP plot for overlaying of different groups. c. UMAP plot for different subsets of monocytes. d. UMAP plots for individual antibody (protein) expression on monocyte populations. Scale bar shows the expression level of protein expression on the cell clusters (blue -lowest and red highest expression; relative expression).

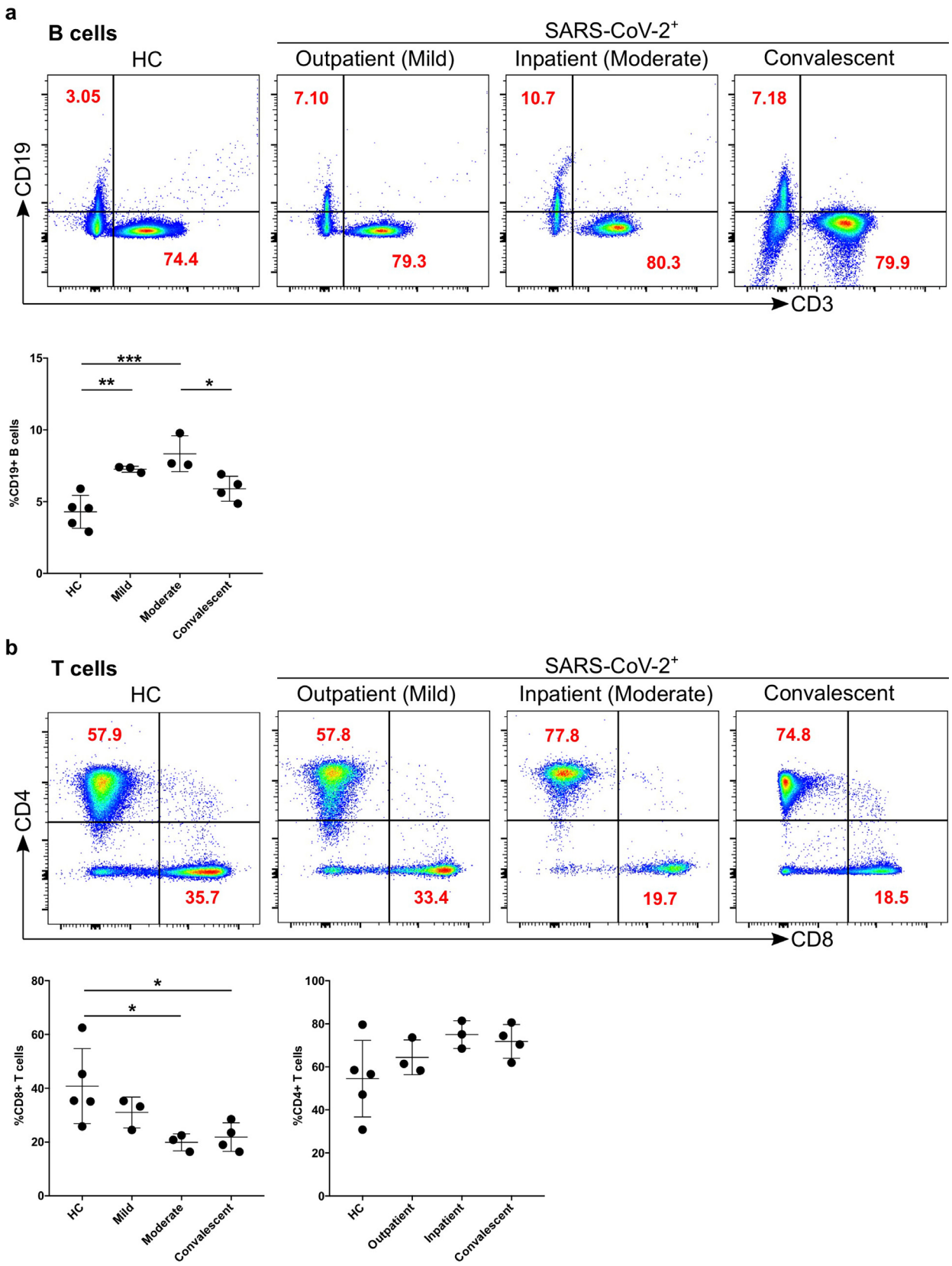

Figure 4. Increased B cells in mild and moderate patients and reduced $CD8^+$ cytotoxic T cells in moderate and convalescent patients. a. The stained PBMCs were gated on lymphocyte population and examined for the CD19 and CD3 expression in HC, mild, moderate and convalescent (upper FACS panel). One exemplary dot plot is shown per study group. The bar diagram shows $CD3^-CD19^+$ B cells. *P-value $\leq$0.05, **P-value $\leq$0.01 and ***P-value $\leq$0.001. b. The $CD19^-CD3^+$ lymphocytes were examined for $CD4^+$ and $CD8^+$ T marker expression. One exemplary dot plot is shown per study group. There was statistically significant difference among HC, moderate and convalescent (upper FACS panel). $CD8^+$ T cells were significantly reduced in moderate and convalescent groups. *P-value $\leq$0.05.

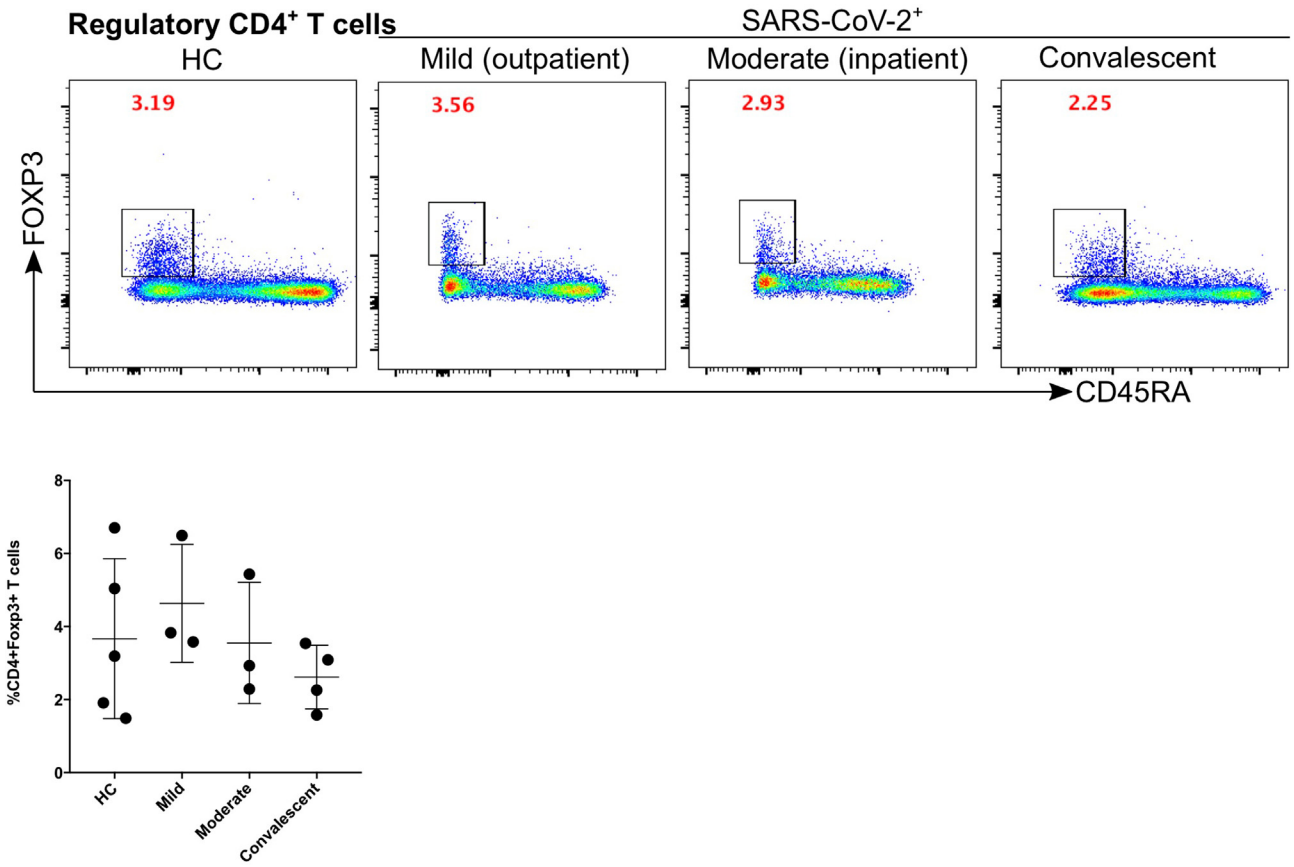

Figure 5. Kinetics of regulatory T cells is not affected significantly in mild, moderate and convalescent patients. Foxp3^{+} expression on CD19^{-}CD3^{+}CD4^{+}CD45RA^{-} T cells to identify the regulatory T cells in HC, inpatient, outpatient and convalescent (upper FACS panel).

2.4. Dynamics of B and T cells in mild, moderate and convalescent patients

Both T and B cells are indispensable for the immune response against viral infections including SARS-CoV-2. Firstly, we compared the number of B cells, which give rise to virus-specific antibodies (see the gating strategy in Figure 1a). The CD19^{+}CD3^{-} cells (B cells) were significantly increased in mild ($p = 0.008$; fold change x1.7) and moderate ($p = 0.0008$; fold change x1.9) patients compared with HC (Figure 4a). B cells were significantly decreased in moderate patients compared to convalescent ($p = 0.04$) group (Figure 4a). Comparing CD3^{+}CD19^{-} lymphocytes among the different patient groups we observed no significant difference. Moreover, CD3^{+} cells were analysed for the CD4^{+} and CD8^{+} T cell compartment. There was a tendency of increased CD4^{+} T cells for mild, moderate, and convalescent patients compared to HC, but no significant difference was observed among any of the groups. CD8^{+} T cells were significantly different between HC compared to moderate ($p = 0.04$) patients or convalescent ($p = 0.04$) group (Figure 4b). Finally, we characterized CD4^{+}FOXP3^{+}CD45R^{-} regulatory T cells (Tregs), however, no significant difference was observed among the different groups (Figure 5).

2.5. Impaired activation and defective cytotoxic functions of CD8^{+} T cells

We found that the percentage of CD8^{+} T cells was decreased in moderate and convalescent patients compared to HC. Thus, we explored the activation status of CD8^{+} T cells based on HLA-DR expression. We found that CD8^{+} T cell activation status (HLA-DR expression) in all three groups of infected patients was significantly different from HC (mild $p = 0.01$, moderate $p = 0.01$, and convalescent $p = 0.01$, Figure 6a). We characterized the cytotoxic potential of CD8^{+} T cells based on granzyme A and perforin levels and found that there was a tendency of decreased granzyme A expression in mild and moderate patients compared with HC (Figure 6b), however, it did not reach statistical significance. Granzyme A^{+}/perforin^{+} expression was significantly decreased in convalescent ($p = 0.02$) group compared with HC (Figure 6b), although mild patients also had reduced levels ($p = 0.07$), it did not reach statistical significance. Furthermore, we studied the expression of CD38, a marker of immune cell activation, which was significantly upregulated in convalescent patients group compared with HC ($p = 0.04$) (Figure 7a). Similarly, convalescent patients group had significantly increased numbers of PD-1^{+} CD38^{+} cytotoxic CD8^{+} T cells compared with HC ($p = 0.006$), moderate ($p = 0.005$) and mild ($p = 0.002$), which reflects the exhaustion and non-responsiveness (anergy) of CD8^{+} T cells (Figure 7b). Overall, our data suggested that CD8^{+} T cells have reduced activation, diminished expression of cytotoxic molecules such as perforin and granzyme A and have a severely exhausted phenotype.

2.6. Dynamics of metabolites production in the mild, moderate and convalescent patient

To establish a putative link between the metabolic state of immune cells and the impaired immune response, PBMCs from all patient groups were subjected to ^{1}H-NMR spectroscopy analysis. We identified and quantified a total of 18 metabolites (Figure 8a). Hereby, unsupervised Principal Component Analysis (PCA) showed that spectral data from mild and moderate patients formed overlapping clusters. However, HC and convalescent patients clustered together (Figure 8b), indicating a strong difference in metabolite levels between an infectious state compared to healthy or recovered groups. Statistical analysis of the four different groups revealed that 15 metabolites showed p-values < 0.05, with the highest significance for metabolites related to energy metabolism (Figures 8c and 9 & Table 2). The data indicate that during infection,

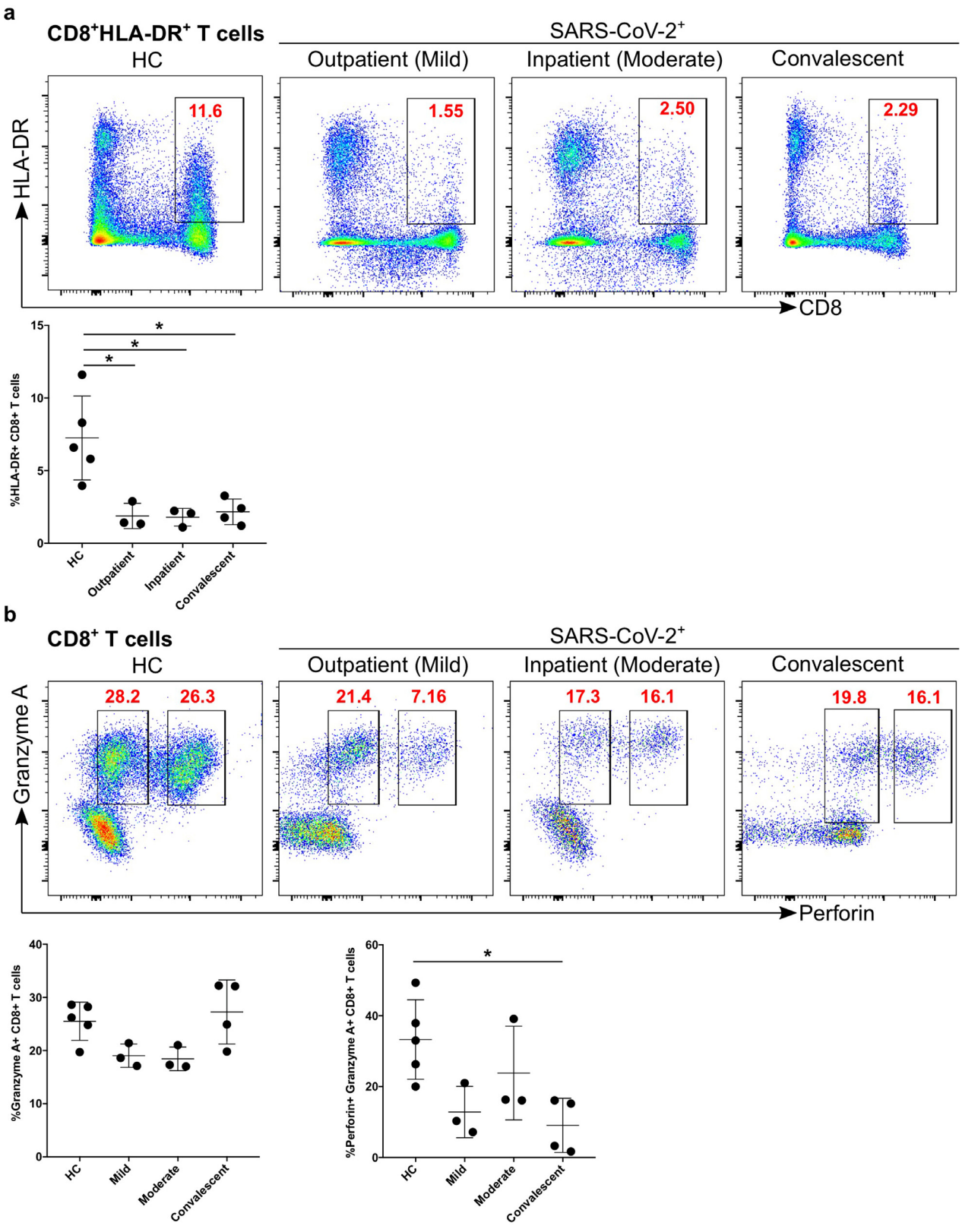

Figure 6. Decreased activation and cytotoxic functional protein expression of $CD8^+$ T cells in convalescent patients group. a. $CD8^+$ T cells were examined for the expression of activation marker HLA-DR (upper FACS panel). One exemplary dot plot is shown per study group. The bar diagram (lower panel) shows that HLA-DR was a significantly lower on $CD8^+$ T cells in mild, moderate and convalescent COVID-19^+ patients compared with HC. *P-value $\leq$0.05. b. $CD8^+$ T cells were examined for the expression of their cytotoxic potential using granzyme A and perforin expression using IC staining (upper FACS panel). One exemplary dot plot is shown per study group. The bar diagram (lower panel; right-hand side) shows that $perforin^+$/granzyme A^+ expression was significantly lower on $CD8^+$ T cells in convalescent group compared with HC, though mild and moderate represent a lower expression of perforin, but it did not reach to a significant level. *P-value $\leq$0.05.

there is a strong consumption (reflecting reduced levels) of glucose, acetate and formate, whilst lactate levels are increased. Furthermore, we also found very high levels of fructose in PBMCs from mild patients, medium concentrations in moderate and, low levels in HC and convalescent patients (Figure 8c). Furthermore, glutamate was almost abolished in mild and moderate patients, potentially as a consequence of enhanced production of α-ketoglutarate in the TCA cycle in PBMCs *via* glutamate dehydrogenase (Figure 8c). Levels of other amino acids such as glycine and isoleucine were low in mild and moderate patients compared with HC, while creatine and alanine were high in mild patient and moderate patient respectively (Figure 8c).

To find an association between different metabolites, we applied the variable importance of projection (VIP) score. We found that formate and glucose had the highest score compared to other metabolites (Figure 10a). To determine if additional metabolites are positively associated with changes in glucose, lactate and fructose, we performed a pattern hunter analysis for all metabolites. We found that high glucose levels correlated with high formate, acetate and glutamate and low lactate and fructose (Figure 10b), indicating enhanced glycolysis and TCA cycle activity in PBMCs. Similarly, fructose, which enters *via* fructose-1-phosphate and dihydroxyacetone phosphate (DAP) into the glycolysis pathway, is correlated positively with lactate and citrate and a decrease in acetate and formate, respectively (Figure 10b). Interestingly, levels of the ROS scavenger taurine are only positively correlated with lactate and fructose, but not glucose (Figure 10c, d).

3. Discussion

SARS-CoV-2 infections are an intense and rapidly evolving area of research due to the ongoing global pandemic [14, 25]. In this study, we used flow cytometry and ^{1}H-NMR to decipher the cell proportions and functional state of immune cells (PBMCs) in mild, moderate and convalescent COVID-19 patients compared to HC. Recent reports from COVID-19 patients suggested that mild and severe patient had lymphopenia [11, 46, 47, 48]. Here, we found that the myeloid cell compartment in PBMCs based on CD16 and CD14 markers suggested that the percentage of non-classical and intermediate monocytes were increased during an active mild or moderate SARS-CoV-2 infection, once infections are cleared the monocyte percentage numbers return to normal. These results are in accordance with some of the recently published studies [49, 50, 51].

In our cohort, specifically CD56^{+}CD8^{+}NK cells were decreased during active SARS-CoV-2 viral infections (moderate), while during recovery the numbers were comparable to HC as reported by others [52]. Similarly, another recent study supports our finding by showing the decrease in the number of NK cell subsets in COVID-19 patients, with no change in CD56^{bright} or CD56^{dim} cells [53]. Furthermore, based on single-cell RNA-sequencing data, a reduced number of NK cells was reported in recovered COVID-19 patients [48]. Thus, altogether, it appears that CD56^{+}NK cells and their subsets could have an important function during the ongoing and clearance of SARS-CoV-2 infections. However, further validation studies are warranted using different *in vivo* model systems with appropriate control groups to pinpoint the exact role of different NK cell subsets in SARS-CoV-2 infection. CD19^{+} B lymphocytes were increased during infection and remain slightly higher than HC, thus reflecting the antibody response against the SARS-CoV-2 virus. Thus, our data suggest that these patients were able to generate SARS-CoV-2 specific B cells, this needs further scientific validation.

A major difference was found in the T lymphocytes compartment. CD8^{+} T cells were significantly decreased in moderate and convalescent patients as reported earlier [52]. Thus, it appears that during viral infection non-virus specific CD8^{+} T cells undergo apoptosis, whilst the viral-specific surviving CD8^{+} T cells are clonally expanded but appeared to have lost their effector functions [54]. To confirm this, we first measured the activation status of CD8^{+} T cells and found that CD8^{+} T cells appeared to be less activated based on their HLA-DR activation marker [26]. Further, CD8^{+} T cells were examined for additional activation marker CD38, which is involved in cell adhesion, signal transduction and calcium signalling [55], was found to be upregulated in convalescent patients but not during active infection. These CD38^{+}CD8^{+} T cells also expressed higher levels of PD-1, which is an immune checkpoint and marker of exhaustion [24, 30, 56, 57, 58]. PD-1 further guards against autoimmunity, stimulates apoptosis of antigen-specific T cells and promotes self-tolerance by suppressing T cell inflammatory activity [59]. Thus, viral infection leaves convalescent patients with exhausted phenotypes. We uncovered that there was not a significant change in the numbers of Tregs in COVID-19 patients, although, there was a trend towards elevated levels of Tregs in COVID-19 patients and reduced Tregs in convalescent patients, in agreement with the previous studies [56].

A key finding of our study was the surprising observation that granzyme A and perforin secreting CD8^{+} T cells were significantly reduced in convalescent patients. These results are in agreement with the recent single-cell transcriptomics analysis which suggests that granzyme B and perforin-1 transcripts were also decreased in convalescent COVID-19 patients compared with moderate or severe illness [60]. In contrast to our results, in young patients, granzyme A or B and perforin levels were increased in mild and moderate cases. Conversely, in elderly COVID-19 patients, there was a reduced expression of granzyme A and perforin [61]. Another study suggested that decreased perforin and granzyme A levels in CD4^{+} T cells, CD8^{+} T cell and NK cells is associated with severely afflicted COVID-19 patients [62]. Furthermore, single-cell transcriptomics analysis of SARS-CoV-2 reactive CD8^{+} T cells in exhausted and non-exhausted subsets were analyzed [63]. These exhausted CD8^{+} T cells were increased in frequency and displayed lesser cytotoxicity and inflammation features in mild COVID-19 patients compared to severe patients [63]. A genetic study performed on two

Table 2. Summary of metabolites dysregulated in PBMCs.

No	Metabolites	HC	Mild	Moderate	Convalescent
1	Glucose	↑↑	↓↓	↓↓	↑↑
2	Formate	↑↑	↓↓↓	↓↓	↑↑
3	Acetate	↑	↓↓	↓	↑
4	Lactate	↓↓	↑↑	↑↑	↓↓
5	Fructose	↓	↑↑	↑	↓
6	Glutamate	↑	↓	↓	↑
7	Citrate	↓	↑↑	↑	↓
8	Taurine	↓↓	-	↑↑	↓
9	Creatine	↓	↑	-	-
10	Alanine	↓	-	↑↑	↓
11	Glycine	↑	↓	↓	-
12	Isoleucine	-	↓↓	↓	↑

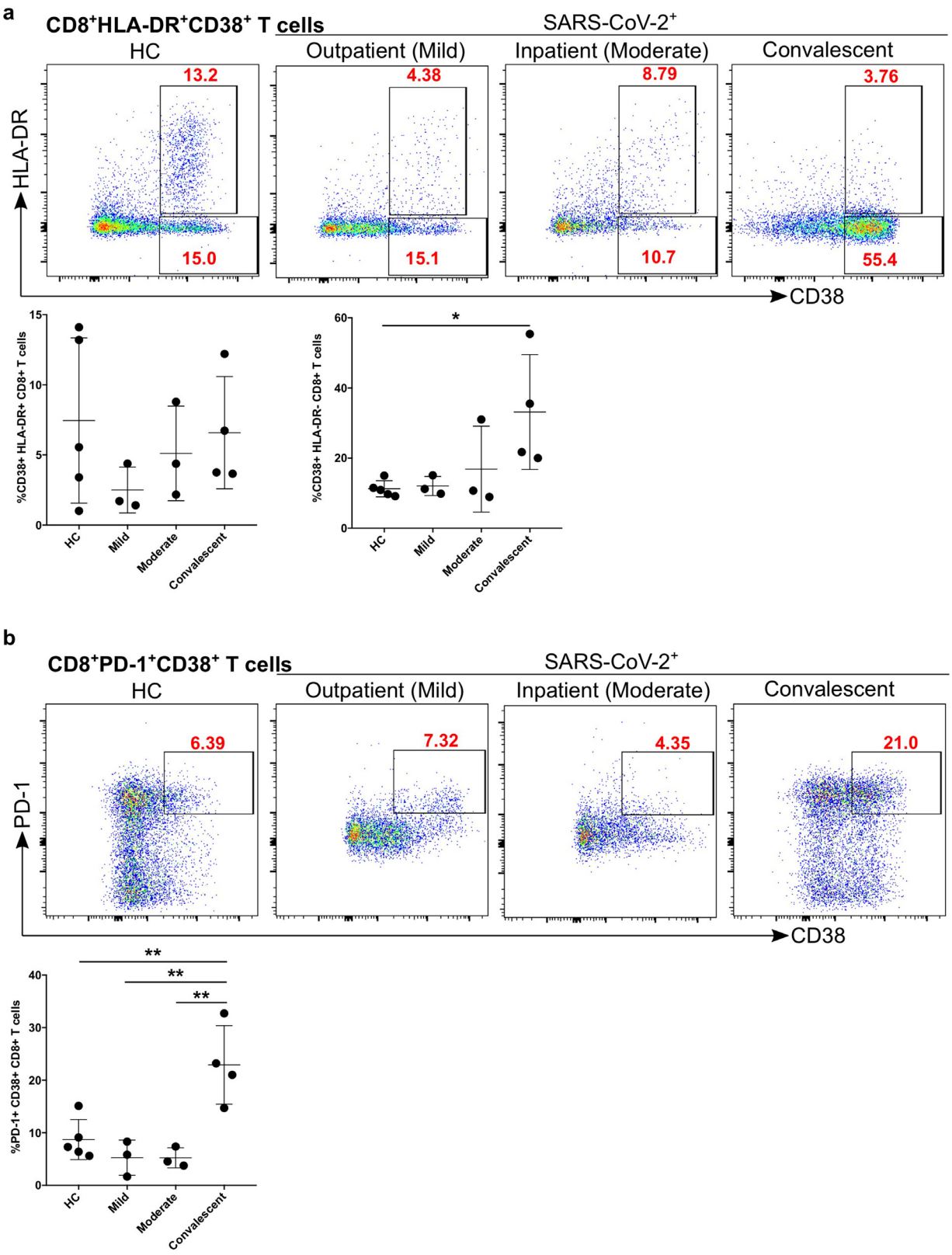

Figure 7. Increased exhausted CD8$^+$ T cells in convalescent patients group. a. Expression of activation marker CD38 on CD8$^+$ T cells (upper FACS panel). One exemplary dot plot is shown per study group. The bar diagram (lower panel) shows that CD38 expression was significantly higher on CD8$^+$ T cells in convalescent COVID-19$^+$ patients compared with HC. *P-value $\leq$0.05. b. Expression of activation marker CD38 and PD-1 on CD8$^+$ T cells (upper FACS panel). One exemplary dot plot is shown per study group. The bar diagram (lower panel) shows that PD-1$^+$CD38$^+$ expression was significantly higher on CD8$^+$ T cells in convalescent group compared with HC. **P-value $\leq$0.01.

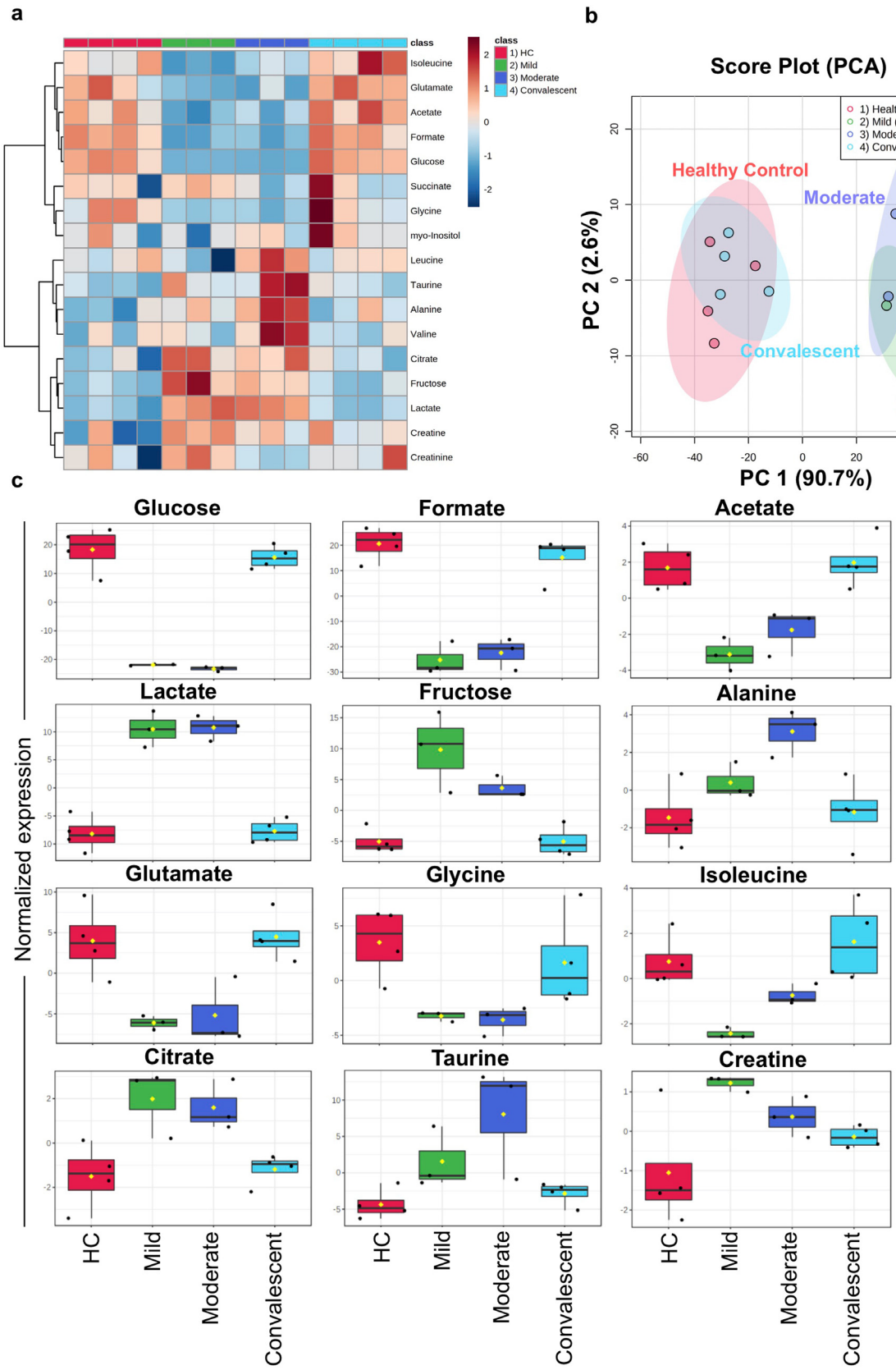

Figure 8. [1]H-NMR spectroscopy of PBMC extracts. a. Heatmap of featured metabolites' concentrations plotted with SARS-CoV-2 progression group clustering. b. Principle component analysis (PCA) was performed to identify the clustering of two different groups. HC and convalescent COVID-19 patient samples cluster together while SARS-CoV-2 infected mild and moderate patients cluster in a separate cluster with PC1: 90.7% and PC2: 2.6%. c. Box plots for differentially abundantly present metabolites in the different group including HC, mild, moderate, and convalescent COVID-19 patient groups. *P-value $\leq$0.05, **P-value $\leq$0.01 and ***P-value $\leq$0.001.

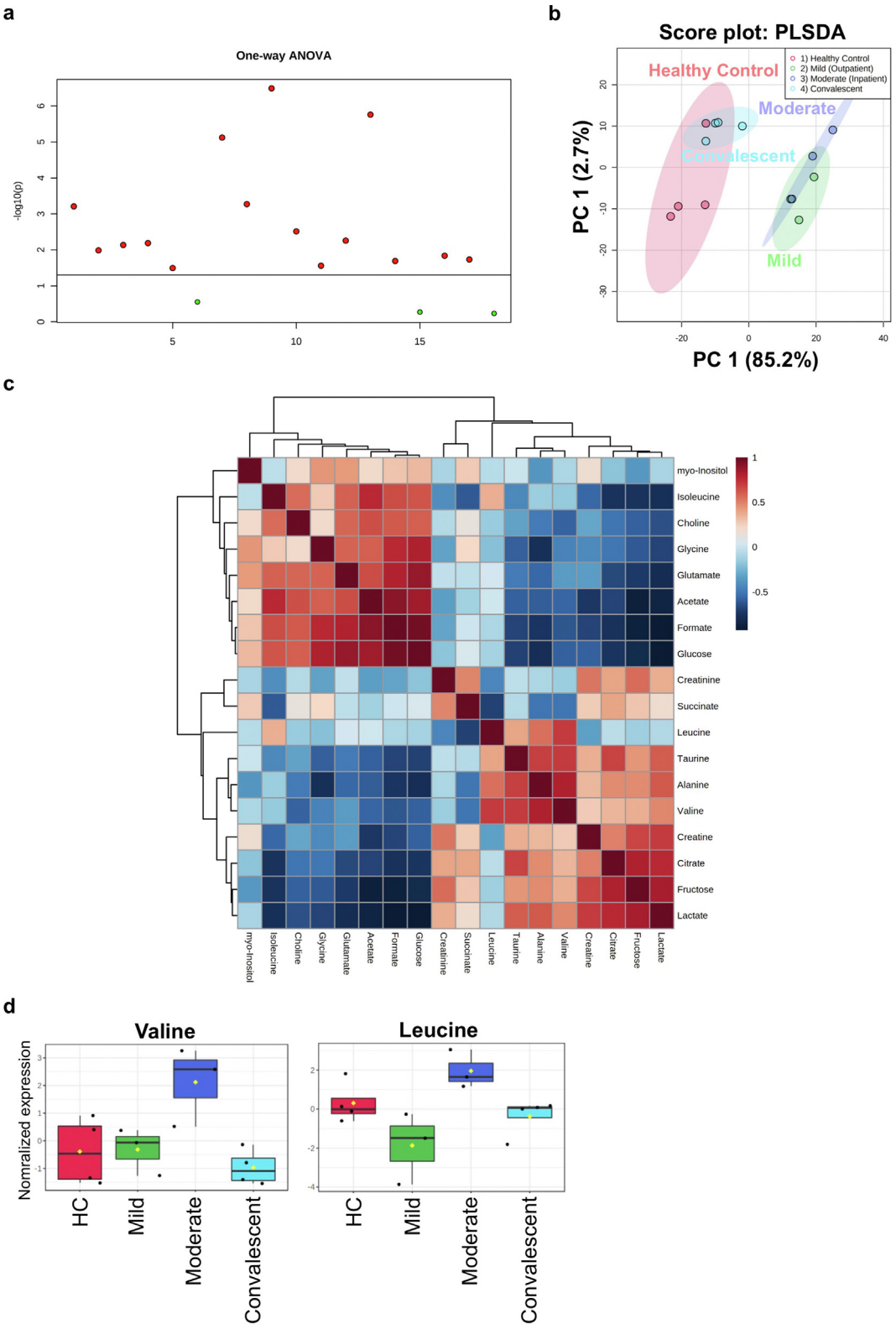

Figure 9. Metabolite analysis in COVID-19 patients. a. Analysis of Variance (ANOVA) for multi-group comparisons. b. Partial Least Squares Discriminant Analysis (PLS-DA) scores plot. c. Hierarchical clustering of metabolites (distance measured with Pearson r correlation coefficient). d. Boxplots for branched-chain amino acids valine and leucine.

Table 3. Antibodies and other reagents used for Flow cytometry.

No.	Product Name	Clone	Fluorochrome	Product ID	Company
NK cells and Monocytes (Panel 1)					
1	CD3	UCHT1	eFluor 450	48-0038-42	Thermofisher
2	CD4	SK3	SuperBright 600	63-0047-42	Thermofisher
3	CD8a	SK1	PerCP-eFluor 710	46-0087-42	Thermofisher
4	CD19	HIB19	eFluor 506	69-0199-42	Thermofisher
5	CD45-RA	HI100	PE-Cy7	25-0458-42	Thermofisher
6	HLA-DR	L243	Alexa Fluor 647	A51010	Thermofisher
7	CD38	HIT2	PE-eFluor 610	61-0389-42	Thermofisher
8	CD56	MEM188	PE	MA119638	Thermofisher
9	CD16	3G8	Super Bright 702	67-0166-42	Thermofisher
10	CD14	61D3	Alexa Fluor 700	56-0149-42	Thermofisher
11	Foxp3 (IC)	PCH101	FITC	11-4776-42	Thermofisher
CD8 exhaustion, T helper follicular cells (Tfh) and antibody-secreting cell (ASC) (Panel 2)					
1	CD3	UCHT1	eFluor 450	48-0038-42	Thermofisher
2	CD19	HIB19	eFluor 506	69-0199-42	Thermofisher
3	CD4	SK3	Super Bright 600	63-0047-42	Thermofisher
4	CD8a	SK1	PerCP-eFluor 710	46-0087-42	Thermofisher
5	CD38	HIT2	PE-eFluor 610	61-0389-42	Thermofisher
6	CD27	O323	Alexa Fluor 700	56-0279-42	Thermofisher
7	CXCR5 (CD185)	MU5UBEE	FITC	11-9185-42	Thermofisher
8	ICOS (CD278)	C398.4A	PE	12-9949-81	Thermofisher
9	PD-1 (CD279)	eBioJ105 (J105)	PE-Cy7	25-2799-42	Thermofisher
10	HLA-DR	L243	Alexa Fluor 647	A51010	Thermofisher
Cytotoxic potential					
1	CD4	SK3	SuperBright 600	63-0047-42	Thermofisher
2	CD8	SK1	PerCP-eFluor 710	46-0087-42	Thermofisher
3	CD19	HIB19	eFluor 506	69-0199-42	Thermofisher
4	CD38	HIT2	PE-eFluor 610	61-0389-42	Thermofisher
5	HLA-DR	L243	Alexa Fluor 647	A51010	Thermofisher
6	GZMA (IC)	CB9	PE	12-9177-42	Thermofisher
7	GZMB (IC)	GB11	Alexa Fluor 488	MA5-23639	Thermofisher
8	Perforin (IC)	dG9	PE-Cy7	12-9177-42	Thermofisher
Other Flow reagents					
1	Ultracompensation bead			01-2222-42	Thermofisher
2	Live/Dead Fixable Near IR staining kit			L10119	Thermofisher
2	FOXP3/TRN FACTOR STAIN BUFFER SET			00-5523-00	Thermofisher
3	FLOW STAIN BUFFER SOLN			00-4222-57	Thermofisher
4	SB COMPLETE STAINING BUFFER			SB-4401-42	Thermofisher
5	DPBS			D8537	Sigma
6	Pancoll human			P04-601000	Pan Biotech

cases highlights the importance of the perforin gene variant A91V which results in the rapid demise in young COVID-19 patients [64]. The possible implication of our finding is that convalescent patients, specifically including cancer patients under treatment, could be susceptible to future opportunistic infections with other viruses including different variants of SARS-CoV-2. However, further, a large cohort study is warranted to understand the potential functions of these molecules (granzyme or perforin) in protection or susceptibility against the COVID-19 infection at gene and function levels.

To date, the general metabolic physiology of PBMCs is not well defined in the literature. However, it is clear now that PBMCs are dependent on circulating nutrients and hormones in the blood [65]. A defective immune response in COVID-19 patients prompted us to investigate the metabolic functions of these immune cells. Our metabolomics data indeed shows that PBMCs from actively infected patients have a distinct metabolic profile from convalescent or healthy individuals. The most notable difference we observed was for metabolites from the glycolysis and oxidative phosphorylation (TCA cycle) pathway, which is in accordance with recently published transcriptome data for PBMCs [39, 43]. Metabolites such as glucose, formate, acetate and choline were also reduced in PBMCs in infected patients whereas, HC and convalescent patients had a normal profile. Accordingly, the glycolytic pathway end products such as lactate were higher in active mild and moderate COVID-19 patients compared with HC and convalescent individuals. Therefore, our data suggest that PBMCs (which constitute a major fraction of T lymphoid cells: 70–80%) may have modulated their metabolic functions, particularly favouring the oxidative phosphorylation pathway over the glycolytic pathway, to meet the high demands of energy needed to combat the ongoing viral infection.

A recent report suggested that elevated glucose levels enhance SARS-CoV-2 replication and cytokine expression in monocytes and glycolysis sustains the viral-induced monocyte response [66]. Recently, it was emphasized that glucose consumption in PBMCs during COVID-19 disease could be also a read-out of cytokine storms [34]. Further, a higher abundance of citrate in PBMCs suggested that perhaps T cells could use the oxidative phosphorylation pathway for energy consumption to

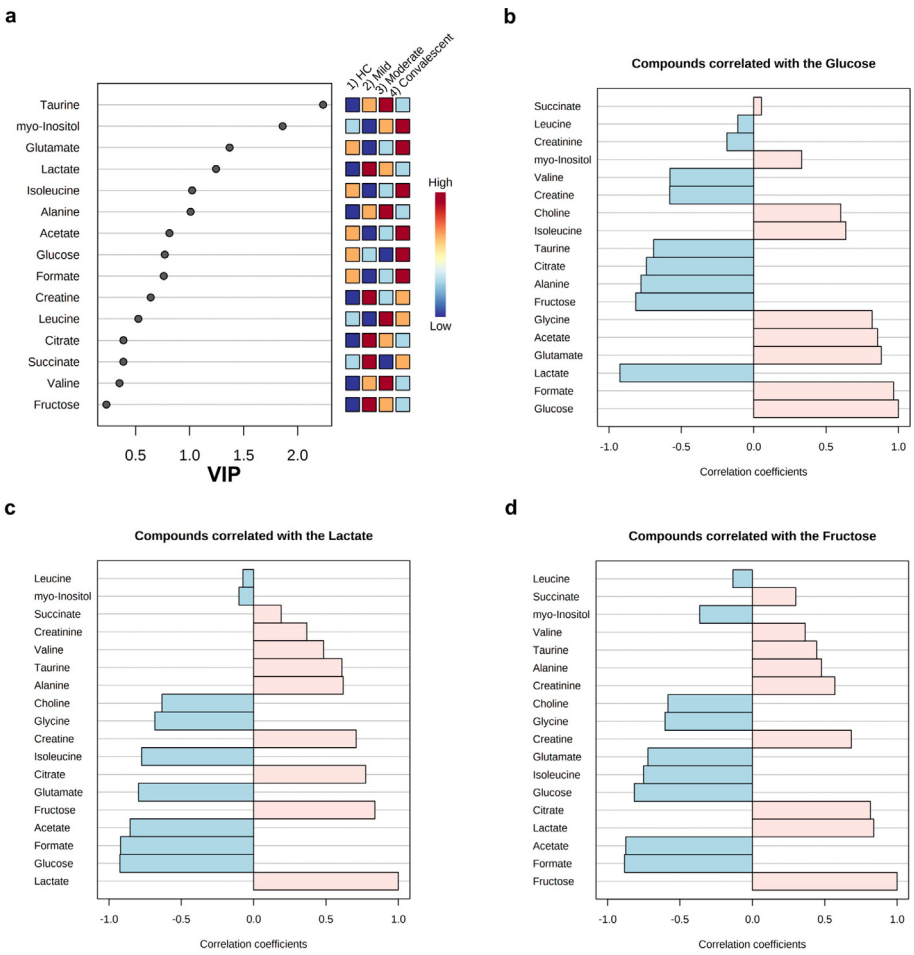

Figure 10. Pattern hunter plots provide an insight of close correlations with other metabolites during COVID-19 infection. a. Variable Importance in Projection (VIP) scores for all metabolites in the four studied groups. b. Pattern hunter plot for glucose. c. Pattern hunter plot for lactate. d. Pattern hunter plot for fructose.

endure the infection, as recent transcriptomic data also suggested that higher expression of genes related to oxidative phosphorylation both in peripheral mononuclear leukocytes and bronchoalveolar lavage fluid (BALF) could play a crucial role in increased mitochondrial activity during SARS-CoV-2 infection [34].

Another remarkable finding of our study was the increase of fructose levels in PBMCs during the course of infection. Previous findings suggested that fructose is involved in the inflammatory pathways for the production of IL-1β and IL-6 production [67]. Thus, it is conceivable that the immune cells (most probably monocytes) could be triggered by higher fructose and simultaneously induce inflammation and IFN-γ production by T cells [67]. These findings correlate with recent transcriptomic studies on the BALF from infected COVID-19 patients and plasma of COVID-19 patients that also identified changes in fructose metabolism [34, 68].

Several amino acids are involved in anti-inflammatory effects, especially arginine, glutamine and glycine appeared to improve lung damage induced by infections [69]. Administration of glutamine reduced the inflammatory cytokines, whereas arginine or glycine reduced IL-6 and CXCL-1 expression in the alveolar epithelium [70]. Additionally, glutamine is an important signalling molecule involved in activating mammalian target of rapamycin (mTOR) signalling which is critical for immune cell activity and inhibiting catabolic functions such as protein degradation and apoptosis [71]. In our study, we found a reduced abundance of glutamate and glycine in PBMCs during the mild and moderate COVID-19 patients. Reduced glucose and glutamine are involved in the hexosamine biosynthetic pathway and could be responsible for poor T cell clonal expansion and function [41]. The exact molecular mechanism of individual amino acids is a complex phenomenon and currently unclear. However, at least in theory, supplementation of glutamine and glycine could be beneficial for COVID-19 patients.

We finally observed a reduction of granzyme A and perforin levels in $CD8^+$ T cells and detected an ambient level of antioxidant amino acid taurine in convalescent patients, which could be involved in the modulation of cytotoxic functions of $CD8^+$ T cells. Both granzyme A and perforin are involved in ROS production and taurine serves as ROS scavenger [72, 73]. Thus, decreased granzyme A and perforin could be implicated in reduced ROS production for the impaired effectiveness of $CD8^+$ T cells in either convalescent patients or COVID-19 patients. This should be the case, as taurine levels are generally increased during active infection in mild/moderate patients compared to healthy controls and are not specifically decreasing due to granzyme A and perforin lacking ROS activity in COVID-19 patients. However, this finding needs further investigation to validate this hypothesis as it is unclear how ROS and taurine act together to affect the cytotoxic functions of immune $CD8^+$ T cells. In summary, the metabolomics data generated in this study provides first and crucial insights into the complex metabolic changes of PBMCs during SARS-CoV-2 infections, warranting further future in-depth investigation.

4. Conclusions

Using immunophenotyping and metabolomics approaches we detected significant changes in PBMC samples of mildly and moderately affected COVID-19 as well as convalescent patients compared with healthy controls. The reduced percentage of NK cells in both mild and moderate patient groups corresponded with the clustering of PBMCs metabolite levels in the principal component analysis distinct from the cluster formed by healthy and convalescent individuals. The dramatically changed metabolic activity and pathways, such as glycolysis and TCA cycle, might not only lead to a vulnerability of COVID-19 patients to subsequent infections but can also offer insights into how PBMCs could be manipulated towards a better survival and personalized treatment of moderate and severe COVID-19 patients.

5. Limitation of the study

The current study is performed from the samples obtained during the first wave of infections and suffers from the limited number of patients used in the study. The use of appropriate controls such as influenza viral infection would have been useful for a more generalized conclusion. Therefore, results obtained in future studies might differ from subsequent waves of infections in new patient cohorts. Further, the novel SARS-CoV-2 variants or vaccine candidates might promote alternative host immune evasion strategies to infect the host, thus, eliciting a different immune response. Nonetheless, this study certainly highlights the importance of distinct cell types as well as the crucial function of cell metabolism during SARS-CoV-2 viral infection and even after recovery.

6. Materials and methods

6.1. Ethics statement

The study protocols were approved by the University of Tübingen, Germany Human Research Ethics Committee (TÜCOV: 256/2020BO2 (convalescent study), COMIHY: (225/2020AMG1) (outpatient study)-COMIHY, EUDRA-CT: 2020-001512-26, ClinicalTrials.gov ID: NCT04340544, and COV-HCQ: (190//2020AMG1) (inpatient study)-COV-HCQ, EUDRA-CT: 2020-001224-33, ClinicalTrials.gov ID: NCT04342221, 556/2018BO2) and all associated procedures were carried out in accordance with approval guidelines. All participants provided written informed consent in accordance with the Declaration of Helsinki.

6.2. Study participants

SARS-CoV-2 positive patients were used for this study and no other virus species were analysed in this study (COMIHY and COV-HCQ). Blood was collected from COVID-19 patients enrolled into two different prospective randomized, placebo-controlled, double-blind clinical trials evaluating the safety and efficacy of hydroxychloroquine in COVID-19 outpatients (COMIHY) and hospitalized patients (COV-HCQ). We analysed subsets of these study cohort and used outpatient (n = 3; COMIHY) which came to a specified outpatient ward at the Institute of Tropical Medicine with mild symptoms and blood was taken and usually defined as D1 outpatients. Inpatients (n = 3; COV-HCQ), blood was taken after 7–9 days after study inclusion defined as D7. These patients had moderate symptoms needing hospital care, however not being transferred to the intensive care unit in the hospital. Furthermore, convalescent COVID-19 patients (n = 4) were defined as positive for serum antibody reactive to SARS-CoV-2 and blood was taken when they visited the Institute of Tropical Medicine for testing of antibody levels. Amongst this cohort, 3 persons reported mild fever for 10–11 days and 1 individual reported no fever but found positive for SARS-CoV-2 antibodies. Blood from healthy controls (n = 5) was obtained from the hospital blood bank.

6.3. Flow cytometry and UMAP data analysis

PBMCs were isolated by the standard Ficoll method [74]. A total of 1–2 x10^6 PBMCs per participants were used for three FACS panels (Table 3). In brief, firstly, to distinguish between live from dead, the cells were incubated with LIVE/DEAD Fixable Infra-Red Dead stain (Thermofisher) for 15 min at room temperature (RT) into 1:40 diluted dye in DPBS. Subsequently, after LIVE/DEAD staining, cells were stained with surface markers in DPBS (Sigma) with Super Bright stain Buffer (Thermofisher) for 30 min at RT. After surface staining cells were also stained for intracellular (IC) markers. Before IC staining, cells were fixed for 30–45 min and permeabilized for 5 min followed by IC antibody incubation for additional 30 min at RT. Cells were washed and resuspended in DPBS containing 2%FBS. Fixing of cells was performed irrespective of whether the panel was used for IC staining or not to prevent the possible contamination during the acquisition of the samples. All the staining procedures were performed in the dark to avoid the photo-bleaching of dyes. For each sample, 200,000 cells were acquired using BD LSRFortessa (core facility) equipped with 4 lasers (violet, blue and yellow-green and Red). Data were analysed using Flow Jo (Tree Star) and fluorescence minus one controls (FMO) were used for setting up the arbitrary gates for the major cell markers. Furthermore, UMAP dimensional reduction analysis was performed using UMAP plug-in [45] in Flowjo software using default setting except for minimum distance (0.2 instead of 0.5) and population (n = 15) as advised by a plug-in. First, dead/debris was removed by gating (FSC-A vs SSC-A; linear scale) then using FSC-A vs FSC-W, we focussed on singlets. The singlets were again gated for live and dead discrimination. An equal number of live cells from each sample (HC, mild and moderate) were concatenated and exported as a single FCS file. This FSC file was subjected to UMAP analysis, each cell population was either monocytes or lymphocytes were again subject to subsequent UMAP analysis for clustering of specific sub-populations. Based on gating or antibodies-stained cells (data-driven) analysis was performed and summarized in Figure 3.

6.4. ^{1}H-NMR metabolomics

To obtain PBMCs metabolites, PBMCs were suspended in an optimized solvent extraction mixture of 9:1 (methanol: chloroform) as described elsewhere in detail [75] and extracted with a focused ultrasound system (Covaris E220, Woburn, USA). The extraction solutions were evaporated to dryness for 4 h in a vacuum concentrator and afterwards pellets resuspended with 45 μL in a 1 mM TSP containing deuterated phosphate buffer. After centrifugation at 20,000 x g for 10 min to remove residual macromolecules, 40 μL of the clear supernatant were transferred to 1.7 mm NMR tubes. Spectra were recorded on ultrashielded 600 MHz spectrometer (Bruker AVANCE III HD, Karlsruhe, Germany) with a triple resonance 1.7 mm room temperature probe. Spectra used for analysis were acquired with a 2h 55min lasting CPMG pulse program. Metabolite annotation and quantification were done with ChenomX NMR Suite 8.3.

6.5. Statistical analysis

Bar diagrams were prepared using GraphPad Prism 6.0. Data shown are means ± SD. FACS data were analysed using one-way analysis of variance (ANOVA) for multiple group comparisons (mild, moderate, convalescent and HC) in GraphPad Prism software. No matching or pairing was used. Assumed Gaussian distribution with equal standard deviations (SDs) for experimental design. The mean of each group was compared with the mean of every other group and Tukey's post-hoc tests for multiple comparisons were employed. P-value considered significantly less than 0.05 or equal. Metabolite concentrations from ^{1}H-NMR analysis were exported as comma-separated value spreadsheet file to MetaboAnalyst 4.0 software, normalized with probabilistic quantile normalization (PQN) and range scaled. Unsupervised principal

component analysis (PCA), a dimensionality-reduction method was used for clustering of all metabolites (PC1 and PC2 only). Multiple groups comparison was performed using one way ANOVA. Multivariate data analysis techniques such as partial least squares analysis (PLS-DA) and variable's importance in the PLS-DA (VIP) score analysis were used to find the correlation among different metabolites and various groups. Hierarchical clustering of all the metabolites was measured and distance measurement was performed with Pearson r correlation coefficient.

Declarations

Author contribution statement

Yogesh Singh, Christoph Trautwein: Conceived and designed the experiments; Performed the experiments; Analyzed and interpreted the data; Wrote the paper.

Rolf Fendel: Conceived and designed the experiments; Performed the experiments; Analyzed and interpreted the data; Contributed reagents, materials, analysis tools or data.

Naomi Krickeberg, Georgy Berezhnoy, Rosi Bissinger: Performed the experiments.

Stephan Ossowski, Madhuri S. Salker, Nicolas Casadei: Analyzed and interpreted the data; Contributed reagents, materials, analysis tools or data.

Olaf Riess: Conceived and designed the experiments; Analyzed and interpreted the data; Contributed reagents, materials, analysis tools or data; Wrote the paper.

The Deutsche COVID-19 OMICS Initiative (DeCOI): Contributed reagents, materials, analysis tools or data.

Funding statement

Yogesh Singh was supported by Ferring Pharmaceutical (Project grant no. D3120767). Rolf Fendel was supported by the German Federal Ministry of Education and Research (BMBF) (BMBF-01KI2052) and the German Federal Ministry of Health (BMG) (BMG-ZMVI1- 1520COR801). Rosi Bissinger was supported by Deutsche Forschungsgemeinschaft (DFG Project no. 426724658). Madhuri S. Salker was supported by the Ferring Pharmaceutical, EKFS, and the Margarete von Wrangell (MvW 31-7635.41/118/3) habilitation scholarship co-funded by the Ministry of Science, Research and the arts (MWK) of the state of Baden-Württemberg and by the European Social Funds. Olaf Riess was supported by Deutsche Forschungsgemeinschaft (DFG project no. 428994620).

Data availability statement

Data associated with this study has been deposited at pre-print server bioRxiv under the doi: https://doi.org/10.1101/2020.09.04.282780.

Declaration of interests statement

The members of the Deutsche COVID-19 Omics Initiative (DeCOI) are Janine Altmüller, Angel Angelov, Anna C. Aschenbrenner, Robert Bals, Alexander Bartholomäus, Anke Becker, Matthias Becker, Daniela Bezdan, Michael Bitzer, Conny Blumert, Ezio Bonifacio, Peer Bork, Bunk Boyke, Helmut Blum, Nicolas Casadei, Thomas Clavel, Maria Colome-Tatche, Markus Cornberg, Inti Alberto De La Rosa Velázquez, Andreas Diefenbach, Alexander Dilthey, Nicole Fischer, Konrad Förstner, Sören Franzenburg, Julia-Stefanie Frick, Gisela Gabernet, Julien Gagneur, Tina Ganzenmueller, Marie Gauder, Janina Geißert, Alexander Goesmann, Siri Göpel, Adam Grundhoff, Hajo Grundmann, Torsten Hain, Frank Hanses, Ute Hehr, André Heimbach, Marius Hoeper, Friedemann Horn, Daniel Hübschmann, Michael Hummel, Thomas Iftner, Angelika Iftner, Thomas Illig, Stefan Janssen, Jörn Kalinowski, René Kallies, Birte Kehr, Andreas Keller, Oliver T. Keppler, Sarah Kim-Hellmuth, Christoph Klein, Michael Knop, Oliver Kohlbacher, Karl Köhrer, Jan Korbel, Peter G. Kremsner, Denise Kühnert, Ingo Kurth, Markus Landthaler, Yang Li, Kerstin U. Ludwig, Oliwia Makarewicz, Manja Marz, Alice C. McHardy, Christian Mertes, Maximilian Münchhoff, Sven Nahnsen, Markus Nöthen, Francine Ntoumi, Peter Nürnberg, Stephan Ossowski, Jörg Overmann, Silke Peter, Klaus Pfeffer, Isabell Pink, Anna R. Poetsch, Ulrike Protzer, Alfred Pühler, Nikolaus Rajewsky, Markus Ralser, Kristin Reiche, Olaf Rieß, Stephan Ripke, Ulisses Nunes da Rocha, Philip Rosenstiel, Antoine-Emmanuel Saliba, Leif Erik Sander, Birgit Sawitzki, Simone Scheithauer, Philipp Schiffer, Jonathan Schmid-Burgk, Wulf Schneider, Eva-Christina Schulte, Joachim L. Schultze, Alexander Sczyrba, Mariam L. Sharaf, Yogesh Singh, Michael Sonnabend, Oliver Stegle, Jens Stoye, Fabian Theis, Thomas Ulas, Janne Vehreschild, Thirumalaisamy P. Velavan, Jörg Vogel, Sonja Volland, Max von Kleist, Andreas Walker, Jörn Walter, Dagmar Wieczorek, Sylke Winkler, John Ziebuhr.

Additional information

The clinical trial described in this paper was registered at ClinicalTrials.gov under the registration number NCT04342221.

Acknowledgements

We thank you all the patients who participated in this study and FACS core facility (Klinikum-Berg) for accessing the Flow cytometry for the experiments. We also give thanks Jana Held and Andrea Kreidenweiss from Institute of Tropical Medicine, Tübingen University for their help with coordination of the clinical trials and proof-reading of the manuscript.

References

[1] N. Zhu, et al., A novel coronavirus from patients with pneumonia in China, 2019, N. Engl. J. Med. 382 (2020) 727–733.
[2] J.C.-L. Dashboard. https://coronavirus.jhu.edu/map.html, 2020.
[3] W.L. Dashboard. https://covid19.who.int, 2020.
[4] L. Chang, Y. Yan, L. Wang, Coronavirus disease 2019: Coronaviruses and blood safety, Transfus. Med. Rev. (2020).
[5] N.J.M.P.J. Lehner, How does SARS-CoV-2 cause COVID-19? Science 510–511 (2020).
[6] J. Liu, et al., Community transmission of severe acute respiratory syndrome coronavirus 2, Shenzhen, China, 2020, Emerg. Infect. Dis. 26 (2020).
[7] T. Singhal, A review of coronavirus disease-2019 (COVID-19), Indian J. Pediatr. 87 (2020) 281–286.
[8] WHO, WHO-2019-nCoV-Sci_Brief-Transmission_modes-2020.3-eng.pdf, WHO Report, 2020.
[9] C. Rothe, et al., Transmission of 2019-nCoV infection from an asymptomatic contact in Germany, N. Engl. J. Med. 382 (2020) 970–971.
[10] Z. Xu, et al., Pathological findings of COVID-19 associated with acute respiratory distress syndrome, Lancet Respir. Med. 8 (2020) 420–422.
[11] Wei Huang, J.B. Michelle McNamara, Suraj Saksena, Marsha Hartman, Tariq Arshad, J. Scott, Bornheimerand Maurice O'Gorman, Lymphocyte subset counts in COVID-19 patients: a meta-analysis, Cytometry A (2020).
[12] G. Chen, et al., Clinical and immunological features of severe and moderate coronavirus disease 2019, J. Clin. Invest. 130 (2020) 2620–2629.
[13] Y. Shi, et al., COVID-19 infection: the perspectives on immune responses, Cell Death Differ. 27 (2020) 1451–1454.
[14] K.S.S. Daniela Weiskopf, Matthijs P. Raadsen, Alba Grifoni, Nisreen M.A. Okba, Henrik Endeman, Johannes P.C. van den Akker, Richard Molenkamp, Marion P.G. Koopmans, Eric C.M. van Gorp, Bart L. Haagmans, Rik L. de Swart, Alessandro Sette, Rory D. de Vries, Phenotype and kinetics of SARS-CoV-2-specific T cells in COVID-19 patients with acute respiratory distress syndrome, Sci. Immunol. 5(48) (2020) eabd2071.
[15] D.M. Del Valle, et al., An inflammatory cytokine signature predicts COVID-19 severity and survival, Nat. Med. 26 (2020) 1636–1643.
[16] Anca Oana Docea, A.T. Dana Albulescu, Oana Cristea, M.V. Ovidiu Zlatian, Sterghios A. Moschos, Dimitris Tsoukalas, Marina Goumenou, Nikolaos Drakoulis, Josef M. Dumanov, Victor A. Tutelyan, Gennadii G. Onischenko, Michael Aschner,

Demetrios A. Spandidos, Daniela Calina, A new threat from an old enemy: Re-emergence of coronavirus (Review), Int. J. Mol. Med. 45 (2020) 1631–1643.
[17] E.Z. Ong, et al., A dynamic immune response shapes COVID-19 progression, Cell Host Microbe 27 (2020) 879–882, e872.
[18] A. Picchianti Diamanti, M.M. Rosado, C. Pioli, G. Sesti, B. Lagana, Cytokine release syndrome in COVID-19 patients, A new scenario for an old concern: the fragile balance between infections and autoimmunity, Int. J. Mol. Sci. 21(9) (2020) 3330.
[19] N. Vabret, et al., Immunology of COVID-19: current state of the science, Immunity 52 (2020) 910–941.
[20] T.P. Velavan, C.G. Meyer, Mild versus severe COVID-19: laboratory markers, Int. J. Infect. Dis. 95 (2020) 304–307.
[21] H. Wu, et al., Clinical and immune features of hospitalized pediatric patients with coronavirus disease 2019 (COVID-19) in Wuhan, China, JAMA Netw Open 3 (2020) e2010895.
[22] S.Q. Du, W. Yuan, Mathematical modeling of interaction between innate and adaptive immune responses in COVID-19 and implications for viral pathogenesis, J. Med. Virol. (2020).
[23] E.J. Giamarellos-Bourboulis, et al., Complex immune dysregulation in COVID-19 patients with severe respiratory failure, Cell Host Microbe 27 (2020) 992–1000, e1003.
[24] T.J. Braciale, Y.S. Hahn, Immunity to viruses, Immunol. Rev. 255 (2013) 5–12.
[25] J.L. McKechnie, C.A. Blish, The innate immune system: fighting on the front lines or fanning the flames of COVID-19? Cell Host Microbe 27 (2020) 863–869.
[26] I. Thevarajan, et al., Breadth of concomitant immune responses prior to patient recovery: a case report of non-severe COVID-19, Nat. Med. (2020).
[27] R.R. De Assis, et al., Analysis of SARS-CoV-2 antibodies in COVID-19 convalescent plasma using a coronavirus antigen microarray, bioRxiv (2020).
[28] Y. Cao, et al., Potent neutralizing antibodies against SARS-CoV-2 identified by high-throughput single-cell sequencing of convalescent patients' B cells, Cell 182 (2020) 73–84, e16.
[29] C. Qin, et al., Dysregulation of immune response in patients with COVID-19 in Wuhan, China, Clin. Infect. Dis. (2020).
[30] J.W. Song, et al., Immunological and inflammatory profiles in mild and severe cases of COVID-19, Nat. Commun. 11 (2020) 3410.
[31] R. Channappanavar, C. Fett, J. Zhao, D.K. Meyerholz, S. Perlman, Virus-specific memory CD8 T cells provide substantial protection from lethal severe acute respiratory syndrome coronavirus infection, J. Virol. 88 (2014) 11034–11044.
[32] H.L. Janice Oh, S. Ken-En Gan, A. Bertoletti, Y.J. Tan, Understanding the T cell immune response in SARS coronavirus infection, Emerg. Microb. Infect. 1 (2012) e23.
[33] P. Bost, et al., Host-viral infection maps reveal signatures of severe COVID-19 patients, Cell (2020).
[34] L.G. Gardinassi, C.O.S. Souza, H. Sales-Campos, S.G. Fonseca, Immune and metabolic signatures of COVID-19 revealed by transcriptomics data reuse, Front. Immunol. 11 (2020).
[35] J.S. Ayres, Immunometabolism of infections, Nat. Rev. Immunol. 20 (2020) 79–80.
[36] S.K. Thaker, J. Ch'ng, H.R. Christofk, Viral hijacking of cellular metabolism, BMC Biol. 17 (2019) 59.
[37] M.M.B. Moreno-Altamirano, S.E. Kolstoe, F.J. Sanchez-Garcia, Virus control of cell metabolism for replication and evasion of host immune responses, Front. Cell Infect. Microbiol. 9 (2019) 95.
[38] S.S. Gupta, J. Wang, M. Chen, Metabolic reprogramming in CD8+ T cells during acute viral infections, Front. Immunol. 11 (2020).
[39] H.M. Shehata, et al., Sugar or fat?-metabolic requirements for immunity to viral infections, Front. Immunol. 8 (2017) 1311.
[40] L.J. Pallett, N. Schmidt, A. Schurich, T cell metabolism in chronic viral infection, Clin. Exp. Immunol. 197 (2019) 143–152.
[41] M. Swamy, et al., Glucose and glutamine fuel protein O-GlcNAcylation to control T cell self-renewal and malignancy, Nat. Immunol. 17 (2016) 712–720.
[42] C.C. Liew, J. Ma, H.C. Tang, R. Zheng, A.A. Dempsey, The peripheral blood transcriptome dynamically reflects system wide biology: a potential diagnostic tool, J. Lab. Clin. Med. 147 (2006) 126–132.
[43] Y. Xiong, et al., Transcriptomic characteristics of bronchoalveolar lavage fluid and peripheral blood mononuclear cells in COVID-19 patients, Emerg. Microb. Infect. 9 (2020) 761–770.
[44] K.L. Wong, et al., The three human monocyte subsets: implications for health and disease, Immunol. Res. 53 (2012) 41–57.
[45] L. McInnes, J. Healy, N. Saul, L. Großberger, UMAP: Uniform Manifold approximation and projection, J. Open Sour. Software 3 (2018).
[46] J. Liu, et al., Longitudinal characteristics of lymphocyte responses and cytokine profiles in the peripheral blood of SARS-CoV-2 infected patients, EBioMedicine 55 (2020) 102763.
[47] F. Wang, et al., Characteristics of peripheral lymphocyte subset alteration in COVID-19 pneumonia, J. Infect. Dis. (2020).
[48] W. Wen, et al., Immune cell profiling of COVID-19 patients in the recovery stage by single-cell sequencing, Cell Discov. 6 (2020) 31.
[49] D. Zhang, et al., COVID-19 infection induces readily detectable morphological and inflammation-related phenotypic changes in peripheral blood monocytes, the severity of which correlate with patient outcome, medRxiv (2020).
[50] A. Silvin, et al., Elevated calprotectin and abnormal myeloid cell subsets discriminate severe from mild COVID-19, Cell (2020).
[51] T. Takahashi, et al., Sex differences in immune responses that underlie COVID-19 disease outcomes, Nature (2020).
[52] Y. Jiang, et al., COVID-19 pneumonia: CD8(+) T and NK cells are decreased in number but compensatory increased in cytotoxic potential, Clin. Immunol. 218 (2020) 108516.
[53] I. Christopher Maucourant, F. Andrea Ponzetta, Soo Aleman, Martin Cornillet, Laura Hertwig Benedikt Strunz, Antonio Lentini, Björn Reinius, Demi Brownlie, Angelica Cuapio Gomez, Eivind Heggernes Ask, Ryan M. Hull, Alvaro Haroun-Izquierdo, Marie Schaffer, Jonas Klingström, Elin Folkesson, Marcus Buggert, Johan K. Sandberg, Lars I. Eriksson, Olav Rooyackers, Hans-Gustaf Ljunggren, Karl-Johan Malmberg, Jakob Michaëlsson, Nicole Marquardt, Quirin Hammer, Kristoffer Stralin, Niklas K. Björkström, the Karolinska COVID-19 Study Group, Natural killer cell immunotypes related to COVID-19 disease severity, Sci. Immunol. 2020 (2020).
[54] B. Diao, et al., Reduction and functional exhaustion of T cells in patients with coronavirus disease 2019 (COVID-19), Front. Immunol. 11 (2020) 827.
[55] E. Katsuyama, et al., The CD38/NAD/SIRTUIN1/EZH2 Axis mitigates cytotoxic CD8 T cell function and identifies patients with SLE prone to infections, Cell Rep. 30 (2020) 112–123, e114.
[56] H.Y. Zheng, et al., Elevated exhaustion levels and reduced functional diversity of T cells in peripheral blood may predict severe progression in COVID-19 patients, Cell. Mol. Immunol. (2020).
[57] R. Zhou, et al., Acute SARS-CoV-2 infection impairs dendritic cell and T cell responses, Immunity (2020).
[58] S. De Biasi, et al., Marked T cell activation, senescence, exhaustion and skewing towards TH17 in patients with COVID-19 pneumonia, Nat. Commun. 11 (2020) 3434.
[59] L.M. Francisco, P.T. Sage, A.H. Sharpe, The PD-1 pathway in tolerance and autoimmunity, Immunol. Rev. 236 (2010) 219–242.
[60] J.Y. Zhang, et al., Single-cell landscape of immunological responses in patients with COVID-19, Nat. Immunol. 21 (2020) 1107–1118.
[61] J. Westmeier, et al., Impaired cytotoxic CD8(+) T cell response in elderly COVID-19 patients, mBio 11 (2020).
[62] A. Mazzoni, et al., Impaired immune cell cytotoxicity in severe COVID-19 is IL-6 dependent, J. Clin. Invest. (2020).
[63] A. Kusnadi, et al., Severely ill COVID-19 patients display impaired exhaustion features in SARS-CoV-2-reactive CD8(+) T cells, Sci. Immunol. 6 (2021).
[64] O. Cabrera-Marante, et al., Perforin gene variant A91V in young patients with severe COVID-19, Haematologica 105 (2020) 2844–2846.
[65] Y. Zeng, et al., Peripheral blood mononuclear cell metabolism acutely adapted to postprandial transition and mainly reflected metabolic adipose tissue adaptations to a high-fat diet in minipigs, Nutrients 10 (2018).
[66] A.C. Codo, et al., Elevated glucose levels favor SARS-CoV-2 infection and monocyte response through a HIF-1 alpha/Glycolysis-Dependent Axis, Cell Metabol. (2020).
[67] N. Jaiswal, S. Agrawal, A. Agrawal, High fructose-induced metabolic changes enhance inflammation in human dendritic cells, Clin. Exp. Immunol. 197 (2019) 237–249.
[68] T.S. Di Wu, Xiaobo Yang, Jian-Xin Song, Mingliang Zhang, Chengye Yao, Wen Liu, Muhan Huang, Yuan Yu, Qingyu Yang, Tingju Zhu, Jiqian Xu, Jingfang Mu, Yaxin Wang, Hong Wang, Tang Tang, Yujie Ren, Yongran Wu, Shu-Hai Lin, Yang Qiu, Ding-Yu Zhang, You Shang, Xi Zhou, Plasma metabolomic and lipidomic alterations associated with COVID-19, Natl. Sci. Rev. (2020).
[69] F. Ferrara, F. De Rosa, A. Vitiello, The central role of clinical nutrition in COVID-19 patients during and after hospitalization in intensive care unit, SN Compr. Clin. Med. (2020) 1–5.
[70] C. Ferreira, et al., Non-obese diabetic mice select a low-diversity repertoire of natural regulatory T cells, Proc. Natl. Acad. Sci. U. S. A. 106 (2009) 8320–8325.
[71] M. Watford, Glutamine and glutamate: nonessential or essential amino acids? Anim. Nutr. 1 (2015) 119–122.
[72] Max W.S. Oliveira, J B M, Marcos R. de Oliveira, Zanotto-Filho Alfeu, A. Behr Guilherme, Ricardo F. Rocha, José C.F. Moreira, Fábio Klamt, Scavenging and antioxidant potential of physiological taurine concentrations against different reactive oxygen/nitrogen species, Pharmaceut. Rep. 62 (2010) 185–193.
[73] L. Cunningham, P. Simmonds, I. Kimber, D.A. Basketter, J.P. McFadden, Perforin and resistance to SARS coronavirus 2, J. Allergy Clin. Immunol. 146 (2020) 52–53.
[74] D.J. Maskus, et al., Characterization of a novel inhibitory human monoclonal antibody directed against Plasmodium falciparum Apical Membrane Antigen 1, Sci. Rep. 6 (2016) 39462.
[75] M.A. Lorenz, C.F. Burant, R.T. Kennedy, Reducing time and increasing sensitivity in sample preparation for adherent mammalian cell metabolomics, Anal. Chem. 83 (2011) 3406–3414.
[76] R. Marimuthu, et al., Characterization of human monocyte subsets by whole blood flow cytometry analysis, J. Vis. Exp. (2018).
[77] P. Autissier, C. Soulas, T.H. Burdo, K.C. Williams, Evaluation of a 12-color flow cytometry panel to study lymphocyte, monocyte, and dendritic cell subsets in humans, Cytometry A 77 (2010) 410–419.
[78] R. Davies, P. Vogelsang, R. Jonsson, S. Appel, An optimized multiplex flow cytometry protocol for the analysis of intracellular signaling in peripheral blood mononuclear cells, J. Immunol. Methods 436 (2016) 58–63.